

Direct measurement of human-cone-photoreceptor alignment

Stephen A. Burns, Shuang Wu, Francois Delori, and Ann E. Elsner

The Schepens Eye Research Institute, 20 Staniford Street, Boston, Massachusetts 02114

Received February 2, 1995; accepted April 14, 1995; revised manuscript received May 11, 1995

We have developed an imaging reflectometer to measure cone-photoreceptor alignment. One makes measurements by bleaching the cone photopigment and imaging the distribution of light returning from the retina, which is illuminated from a small source imaged in the plane of the eye's pupil. If the source is near the optimal entry pupil position as determined psychophysically, the distribution of light returning from the retina is peaked, and the magnitude of the peak depends on the location of the source in the pupil of the eye. If the source is far from the optimal entry pupil position, then there is no measurable peak. The location of the peak varies across individuals and coincides with the reported location of best visibility of the measuring light and with previous psychophysical and reflectometric measurements of the Stiles-Crawford peak. The source of this directionality must arise either from the photoreceptors or from behind the photoreceptors because the peak is not present if measurements are made when the cone photopigments have high optical density.

Key words: photoreceptors, color vision, waveguides, visual sensitivity, Stiles-Crawford effect.

1. INTRODUCTION

The cone photoreceptors of the human retina are usually most sensitive to light entering the eye from the center of the pupil.¹ This differential sensitivity is generally attributed to the alignment of the cone outer segments toward the center of the pupil^{1,2} and to the fact that the cones act as waveguides, collecting light from a restricted angular extent and directing the incident light along the outer segments. This alignment is thought to decrease sensitivity to intraocular stray light and to improve the resolution of the eye by increasing sensitivity to light coming from the center of the pupil,³ where the optical quality is optimal.^{4,5} The normal alignment of the photoreceptors toward the pupil of the eye can be altered by a number of retinal diseases,⁶⁻¹⁰ and alignment has been shown to result from a dynamic process.^{8,11-13} If the normal alignment is disturbed by disease, it can recover after resolution of the underlying problem. Thus, improved techniques for measuring photoreceptor alignment are of interest for studying both the relation between photoreceptor structure and function in normal observers and the effect of retinal pathology on photoreceptor function.

In the current paper we describe a technique for optical measurement of the directionality of the cone photoreceptors. The principle of optical reversibility states that a waveguide that accepts light impinging upon one end of a waveguide from a given angular distribution will emit light traveling along the waveguide in the other direction with the same angular distribution. For the photoreceptors this means that, if light is accepted from a preferential angle when it arrives at the cones from the pupil, then light that has been reflected or scattered back into the photoreceptor outer segments from deeper retinal layers will be emitted into the same angle when it emerges from the cones and will thus be directed back toward the pupil. This effect is shown schematically in Fig. 1. When the retina is illuminated there are three

principal components of light that return back out of the eye, although there are actually multiple sources of reflections, scattering, and absorption in the fundus.¹⁴⁻¹⁸ The first component arises from light that enters the cones, is guided through the outer segment, is backscattered or reflected at the base of the outer segment, and is then guided back through the photoreceptors to the pupil (the guided component). The second component is light that has been scattered in the retina and in the choroid. The third component results from a specular reflection from the inner limiting membrane, which, because of the curvature of the foveal pit, forms in the foveal region an image of the source close to the retina.^{19,20} For these last two components a portion of the returning light will intersect the pupil, and thus, from the outside, the pupil will appear to be uniformly illuminated. Thus, by measurement of the spatial distribution of the light emerging from the pupil when the retina is illuminated, it is theoretically possible to measure the directional properties of the human photoreceptors²¹ because the guided portion of the light fills only a portion of the pupil, whereas the other two components fill the entire pupil.

Krauskopf²² first used a reflectometry technique for measurement of photoreceptor alignment but found that his reflectivity measurements were too variable over time. However, by making measurements before and after photopigment bleaching, he was able to demonstrate that the change in reflectance with bleaching was due to the directional properties of the photoreceptors. This optical technique has been refined by van Blokland and Norren^{23,24} and by Gorrard and Delori,²⁵⁻²⁷ and the contribution of photoreceptors to the directional reflectance of the retina is well established.^{22,24-26} Optical techniques give similar information to the more traditional psychophysical methods,^{11,28,29} although the quantitative relation between the two types of measurement has not yet been resolved.^{2,30,31} Although similar in principle to the approach used by van Blokland²³ and by Gorrard

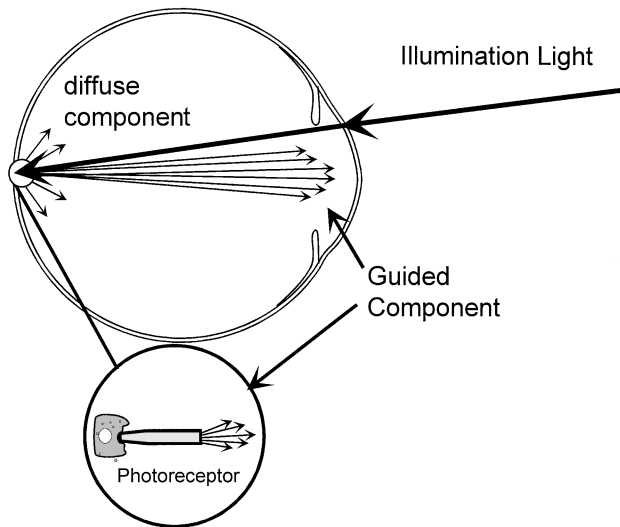


Fig. 1. Schematic diagram of the concept underlying the method described. A waveguide will re-emit light into the same solid angle for which it accepts light. Thus, if we illuminate a photoreceptor (see inset), light will traverse the outer segment, be scattered near the tip of the outer segment, and be captured again by the outer segment. This light will be guided back toward the pupil when it emerges from the photoreceptor inner segment, producing a directional reflection (guided component). In addition, some light will be scattered such that it is not captured by the outer segments. This light will be more uniformly distributed, and a portion will intercept the pupil, producing a diffuse component to the final image of the pupil.

and Delori,²⁵ our implementation involves imaging the entire output distribution of light in the pupil for any given pupil entry position. Thus we can obtain a full two-dimensional intensity distribution of the exit distribution of light for a single entry position. We present initial

results obtained by this technique and examine the effect of photopigment bleaching and polarization on these measurements.

2. METHODS

A. Apparatus

We have modified the apparatus of Gorrand and Delori²⁵ to permit imaging of the distribution of light emerging from the pupil for a single pupil entry position. This provides (1) quantitative measurements of the entire distribution of light in the plane of the pupil, which results from illumination of the retina from a well-controlled pupil entry position; (2) on-line monitoring of the subject's pupil by means of a television system and infrared illumination; and (3) imaging of the retina to control the region of retina being studied.

The optics for illumination and for detection are schematized in Fig. 2. A 543-nm, He-Ne laser provides the illumination. The laser is focused on a pinhole that acts as a spatial filter, removing speckle from the beam. Light from the pinhole of the spatial filter is then collimated by a lens L_1 . Adjacent to lens L_1 is an aperture A_1 that is optically conjugate to the retina. L_1 is mounted on a stage that can be translated perpendicular to the beam by use of two yoked, computer-controlled stepping motors. Thus, when L_1 is moved, the image of the retinal stop (A_1) remains fixed, but the location of the source in the plane of the pupil moves. Lenses L_2 and L_3 are mounted apart from each other at a distance equal to the sum of their focal lengths; thus they relay the collimated image of the spatial filter. They are mounted on a platform that can be translated parallel to the direction of the light. Thus one can focus aperture A_1 on the retina

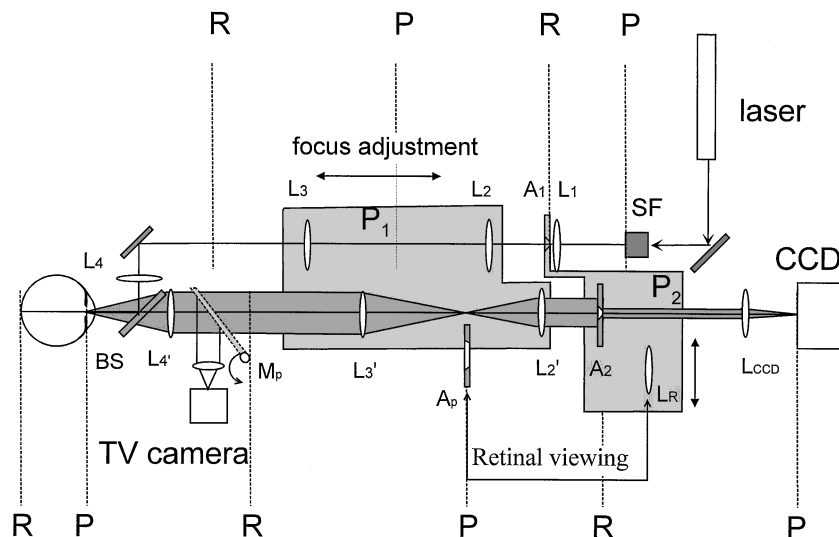


Fig. 2. Schematic of the apparatus (see also Subsection 2.A). The apparatus has both an illumination channel (top) and a detection channel (bottom). Light is provided by a 543-nm He-Ne laser. The laser is focused on a spatial filter located in a pupil conjugate plane (P_1). Light from the spatial filter is collimated by lens L_1 , which is mounted on a computer-controlled stage that can be moved orthogonal to the optical path in two dimensions. Lenses L_2 and L_3 are mounted on a platform that can be translated parallel to the optical path, allowing the experimenter to focus aperture A_1 on the subject's retina. The detection path is arranged similarly, with the surface of the CCD detector located conjugate to the subject's pupil. The experimenter can move a second platform (P_2) on which are mounted apertures A_1 and A_2 and lens L_R . When this platform is moved the two retinal conjugate apertures are moved out of the optical channel, and lens L_R is inserted. This places the CCD conjugate to the retina. A calibrated reticle (not shown) is inserted into the optical channel in place of aperture A_2 , allowing the experimenter to determine the location of the measurement field on the retina. For retinal viewing it is also necessary to insert a pupil conjugate aperture (A_p). This aperture is mounted on a computer-controlled rotary solenoid and serves to block the corneal reflex, permitting higher-contrast views of the retina.

by moving lenses L_2 and L_3 as a pair. This movement does not change the location of the image of the pinhole in the plane of the eye's pupil. Finally, lens L_4 images the pinhole in the pupil of the eye.

Light emerging from the eye follows a similar pathway. A beam splitter (BS) separates the illumination and detection channels. The image of the pupil is collimated by lens L_4' and is relayed by lenses L_3' and L_2' . The retina is imaged at aperture A_1 . Lenses L_3' and L_2' are mounted on the same slide as lenses L_3 and L_2 ; thus, when aperture A_1 is focused on the retina, the retina is focused on aperture A_2 . Aperture A_2 acts as a confocal aperture, limiting the pupil image to light originating from the retinal area illuminated by aperture A_1 . This effect decreases the contribution of the Purkinje images to the pupillary measurements. Finally, lens L_{CCD} images the pupil on the faceplate of the charge-coupled device (CCD). The two retinal conjugate apertures A_1 and A_2 are mounted on a second slide together with a lens L_R . By moving this slide perpendicular to the optical channel the retina conjugate stops (A_1 and A_2) can be removed, and the lens L_R is inserted into the optical channel. In this position L_R is located one focal length from the retinal-image plane and acts to collimate the retinal image, which is then imaged on the face of the CCD. To image the retina we also insert a pupillary conjugate stop A_p . This stop selects light from the central 2 mm of the pupil. By locating the entrance pupil outside this region we can move the corneal reflex outside the central 2 mm of the pupil and can obtain an image of the retina without the contribution of veiling glare from the corneal reflex.

The subject's pupil position can be monitored with a solid-state television camera by actuation of a solenoid that inserts a mirror (M_p) into the detection channel. For pupil monitoring an infrared light-emitting diode under computer control provides diffuse illumination of the orbital region, allowing us to check eye position without altering photopigment regeneration.

The distribution of light in the pupil is measured with a cooled CCD camera (Princeton Instruments). This camera is capable of imaging at a resolution of 512×512 pixels, with an image depth of 16 bits (65,536 gray levels)/pixel, and a pixel size (referenced to the pupil) of 0.025 mm. In practice we do not use the full resolution of the camera but rather combine the output of adjacent pixels (binning). Binning is accomplished by the CCD hardware controller, which allows the charge of neighboring pixels to be combined on the CCD chip itself (binning) prior to reading of the data into the computer. This on-chip binning reduces the readout noise associated with each measurement to approximately that which is associated with the reading of a single pixel. We vary the number of pixels binned according to the experiment being performed, but typically we combine areas of 3×3 pixels, giving a resolution (referenced to the pupil) of 0.075 mm/pixel. The CCD can also be programmed to integrate light over time, and we typically use a 4-s integration time. Data are read into the computer from the CCD at 50 kHz.

B. Corneal Reflex

The largest potential artifacts in our measurements are the Purkinje images of the entrance pupil. The largest

of these is the first Purkinje image (the reflection from the cornea-air interface), which is located close to the pupillary plane.³² With the confocal stops (A_1 , A_2) in place, the first Purkinje image is still often 10–100 times brighter than the light returning from the retina. If the tails of the light distribution of the corneal reflex extend over a considerable distance, then they could significantly distort the measurement of photoreceptor directionality. We examined the significance of this artifact in three ways. First, we measured the light distribution of the corneal reflex for a model eye. The front surface of the model eye was formed by a 40-diopter contact lens, which is similar in power to the human cornea. The contact lens was glued to a water bath filled with a water-india-ink solution. Thus, when the model eye was illuminated, the main component of light reflected from it originated at the air-glass interface, with minimal contributions from other surfaces. We placed the model eye in the optical system and imaged the resulting intensity distribution. The resulting light distribution dropped to less than 0.01 of its peak value within 0.5 mm of the location of the peak intensity, whereas the retinal distribution typically decreased to approximately 0.95 of its maximum within this distance. The results of two other approaches involving illumination of the retina with plane-polarized light and the effect of photopigment bleaching are discussed below, but they support the hypothesis that the guided portion of our measurements arises from properties of the photoreceptors, and they cannot be attributed to imaging of the tails of the corneal reflex.

C. Subjects

Nine subjects were used in this research (four males and five females). Their ages were between 23 and 60 years. All the subjects had normal vision, although one subject had deuteranomalous color vision. Subjects' eyes were dilated with 1% tropicamide prior to performance of measurements, and subjects' pupils had to be at least 6 mm in diameter before participation in the study was permitted. All the human-studies protocols were approved by the Schepens Eye Research Institute's Institutional Review Board.

D. Stimulus

In all the experiments reported here a 2-deg-diameter region of the retina (determined by A_1) was illuminated, and the light returning from the central 1-deg-diameter region (determined by aperture A_2) was used for the measurement. The size of the illumination light at the pupil is determined by the image of the pinhole and is nominally 28 μm in diameter, although blurring increases this value slightly. The maximum illuminance of the measuring light is 5.3 log photopic trolands (Td). The safe time for continuous exposure to this illuminance and to this wavelength is greater than 1 h for all the field sizes, and for our standard 2-deg measuring condition the safe time is greater than 8 h.³³

E. Measurements: Correction for Dark Level and Transmission of the Optics

To compute the directional reflectance of light returning from the retina at a given angle we require three sets of data: (1) the amount of noise and dark current contributed to the measurement by the CCD in

the absence of light, (2) the spatial uniformity of transmission of the optics of the detection channel, and (3) the actual reflectance data. We obtain an estimate of the dark current by making a measurement when all the CCD parameters are set to their experimental values (integration time and the amount of binning), but with the camera shutter closed. The resulting image is composed of the dark level in the CCD (which is minimized by cooling) and of noise fluctuations. We measure the transmission of the detection channel by placing the port of an integrating sphere, illuminated by incoherent light, at the pupillary plane. The integrating sphere generates a uniform source at the entrance of the detection channel. We then measure the spatial distribution of light arriving at the CCD. In general, the transmission of the optics was uniform to within 5%. This calibration also accounts for any simple gain changes between CCD pixels. These two measurements are combined with the CCD image of the eye's pupil to compute the distribution of light emerging from the pupil as

$$L_{\text{pupil}} = \frac{(L_{\text{CCD}} - L_{\text{dark}})}{L_{\text{white}}}, \quad (1)$$

where L_{pupil} is the computed spatial distribution of light emerging from the pupil for a given entry position, L_{CCD} is the measured distribution of light at the CCD, L_{dark} is the average dark current, and L_{white} is the spatial distribution measured with the integrating sphere.

F. Typical Measurement Sequence

In each experimental session we first dilate the subject's pupil and then align the subject's eye to the apparatus by means of a bite bar mounted on an *XYZ* positioning stage. An auxiliary infrared camera displays an image of the eye on a television monitor, on which we indicate the position of the center of the illumination and detection channels. The television camera is mounted in the detection channel prior to aperture A_2 and has only a shallow depth of focus (<1 mm). The proper positioning of the eye at the focal point of lens L_4 is achieved when the image of the pupil is in optimal focus. We then focus the retinal aperture on the subject's retina by moving the focusing platform. This can be done either by imaging the retina and bringing it to best focus or, in most of the cases reported here, by asking the subject to make the adjustment for the subjective best-focus position. Both techniques have been shown to produce the same plane of focus.³⁴

Once both the pupil planes and the retinal planes are optimally adjusted, we turn on the measuring light at a retinal illuminance of 5.3 log Td and allow more than 10 s for bleaching. Next we obtain a series of images, moving the entry pupil position in 1-mm increments. The measuring light is left on continuously to maintain the retina in a bleached state. In general, we can perform a complete measurement sequence (excluding making the bite bar and administering informed consent) in approximately 10 min. If we are testing other retinal locations we can either (1) move a fixation point a known distance or (2) image the retina and have the subject move his or her fixation until the measuring area is aligned with the test region.

G. Bleaching

The effects of changing the density of the cone photopigments were measured by comparison of the distribution of light in the pupil measured when the eye was dark adapted to that measured when it was fully bleached. We first performed a normal measurement series to identify the location for optimal pupil entry. After locating the entry positions of interest, we extinguished the measurement light and dark-adapted the subject for at least 6 min. After dark adaptation a 3.6-log-Td measuring light was turned on, and the reflectance distribution was measured for an entry pupil position near the peak of the high-illuminance reflectance distribution. To make measurements at this relatively low retinal illuminance we programmed the CCD to bin pixels in either a 4×4 or a 8×8 configuration and integrated for 8 s or more. After making the dark-adapted measurement, we increased the test stimulus to 5.2 log Td for 6 min and made another measurement. Finally, we decreased the measurement illuminance back to 3.6 log Td and immediately made another measurement. Thus we obtained two measurements under identical optical conditions, with the exception that the first was made prior to bleaching and the second was made after a strong bleaching stimulus.

H. Polarization

The relation between the polarization of light illuminating the eye and the polarization of light in the plane of the pupil was measured by insertion of a fixed linear polarizer into the illumination channel and a second linear polarizer (the analyzer) into the detection channel. The angle of the analyzer was systematically varied, and the distribution of light in the subject's pupil was measured.

I. Computations

The measured intensity distribution has three main components: reflections from the anterior surfaces of the eye (primarily the corneal reflex but also reflections from other surfaces), the guided component of the light returning from the retina (light guided by the photoreceptors; see Fig. 1), and a diffuse component of the light returning from the retina, which may be due to scattered light that is not passing through the photoreceptors as it emerges from the eye. Our optical design decreases the importance of the anterior reflections for our data, but we discuss their potential contributions below. We model the directed component of the light as having a circularly symmetric Gaussian distribution (see Gorrard and Delori²⁵). We model the diffuse component as a uniform background light that fills the pupil. We estimate parameters for the directed and the diffuse contributions, using a fitting program written in MATLAB (Mathworks, Inc., Natick, Mass.).

To fit the data we first interactively examine the corrected intensity profile of the image. In such a profile the edges of the pupil and the corneal reflex are readily detected. We set cutoff criteria for both the maximum and the minimum valid data. An appropriate maximum data cutoff excludes the majority of the corneal reflex but leaves the light returning through the pupil. An appropriate minimum valid data level includes all the light returning through the pupil but omits fluctuations in the dark level that are present for the region imaged beyond the pupil margins. We then fit the intensity distribution

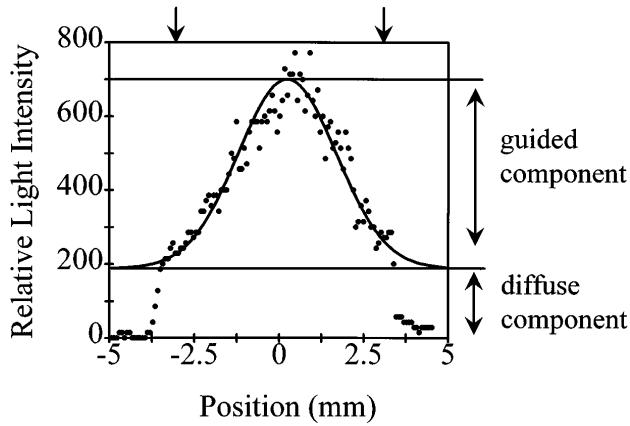


Fig. 3. Cross section of a single measurement obtained for a pupil entry position near the peak of the photoreceptor alignment distribution. The measured intensities (data points) are plotted for a single horizontal row of pixels. The computer-determined best fit for the same row is also shown (curve). The fit was obtained for the entire two-dimensional array of measurements. The computer-determined amplitudes of the diffuse and guided components of the intensity distributions are shown as horizontal lines. The arrows at the top of the graph indicate the pupil margins. This section was chosen such that it does not include the corneal reflex.

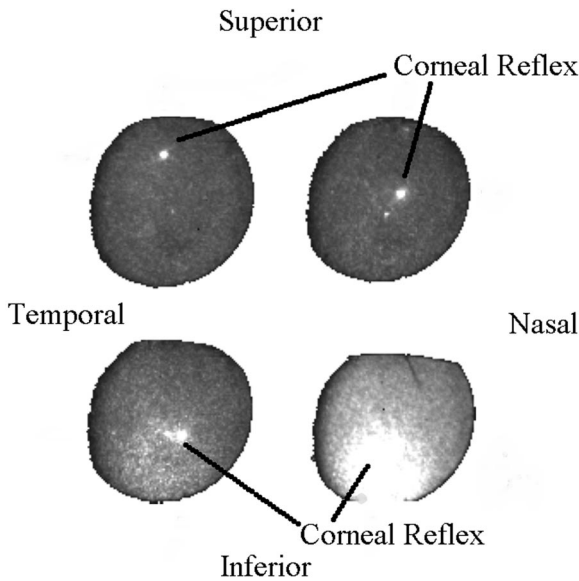


Fig. 4. Four pupillary images obtained for different pupil entry positions for a single subject. The bright dot, which is most visible in the upper two images, shows the location of the corneal reflex. The centrally located bright spot in each image is the fourth Purkinje image. As the entry position of the illumination light is moved toward the inferior central portion of the pupil (bottom row), the total amount of light returning from the retina increases markedly (bottom right). The increase is sharply peaked when the illumination beam enters through a particular region of the pupil (bottom right). It is not possible to print accurately the total dynamic range of the images; however, all four images were identically scaled and printed.

with the sum of a Gaussian and a constant,²⁵ using a simplex least-squares-error minimization. In this fit the Gaussian distribution represents the directed portion of the light returning from the retina, and the constant represents the diffuse component. The predicted intensity surface can be expressed as

$$L_{pupil} = B + A10^{-sd}, \quad (2)$$

where A is the intensity of the guided component, B is the intensity of the diffuse component, s is the space constant of the Gaussian fit to the directed component (in mm^{-2}), and d is the distance in millimeters from the peak of the intensity distribution (x_0, y_0) , computed as $[(x_0 - x)^2 + (y_0 - y)^2]^{1/2}$. A plot of a cross section of a typical data set, together with the computer-determined best fit, is presented in Fig. 3. The fit shown was made to the entire two-dimensional distribution, but we show a cross section through the peak for illustrative purposes. In general, this simple model accounted for between 70% and 90% of the variance of the data when the entry pupil was located near its optimum position.

3. RESULTS

The amount of light returning to the detector depends on where the entry pupil was positioned in the pupil of the eye. Figure 4 shows typical measurements obtained for four pupil entry positions in a normal subject. In these images the small bright spots mark the location of the corneal reflex, which in turn is close to the position at which the illumination beam enters the eye and thus is a convenient marker for the position at which the illumination beam entered the pupil for each image. To facilitate comparison of the amount of light returning to the detector, the intensity ranges of all four measurements were truncated identically to generate the composite image. There was a systematic variation in the pupillary distribution of the retinal reflectance as we varied the entry position. For this subject, when the entry position is in the superior portion of the pupil, there is only a diffuse reflectance that uniformly illuminates the pupil, other than the corneal reflex and traces of the fourth Purkinje image. When the entry position is in the inferior portion of the pupil, the amount of light reflected from the retina increases. This dependence of the amount of light emerging from the eye on the entry position of the illumination light has been found in all subjects measured to date, although there are individual differences in the location of the reflectivity peak.³¹ The location of

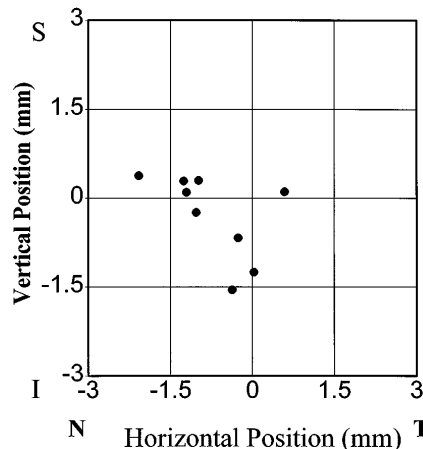


Fig. 5. Location in the plane of the pupil of the computer-determined peak of the guided component for the nine subjects whose responses are reported in this study. This location is hypothesized to be the point in the pupil toward which the foveal cone photoreceptors are oriented. Portions of the pupil: S, superior; I, inferior; N, nasal; T, temporal.

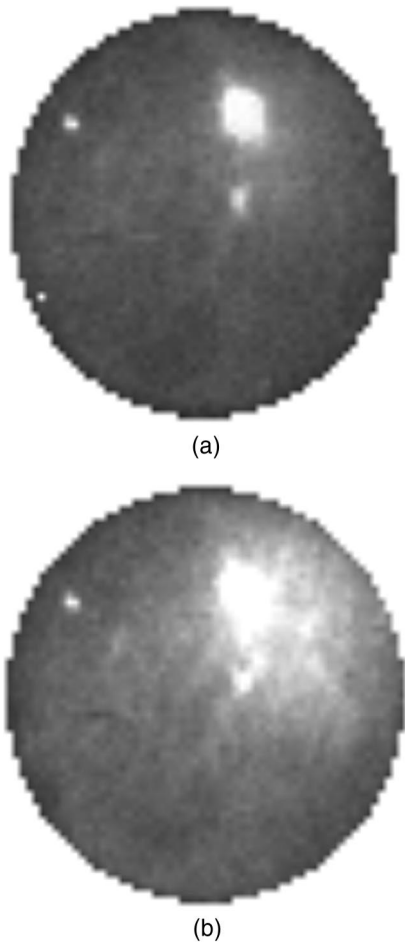


Fig. 6. Comparison of the light distribution measured in the plane of the pupil for identical illumination conditions for a single subject. (a) Dark adapted, (b) bleached. The only difference between these two images is that (a) was obtained after dark adaptation and photopigment regeneration, whereas (b) was obtained after exposure to a bright bleaching light. The bright spot at approximately one o'clock in (a) is the corneal reflex and marks the location at which the measurement light enters the pupil. The fourth Purkinje image is also visible in the center of the pupil. (a) and (b) were identically scaled and printed.

the peak, i.e., the maximum of the guided component, is shown in Fig. 5 for nine subjects. Locations are relative to the center of the pupil. The average space constant [s in Eq. (2)] fitted to the foveal data for nine observers was $0.083 \pm 0.013 \text{ mm}^{-2}$.

A. Effect of Bleaching

We hypothesize that the variations in reflectivity shown in Fig. 4 are due to photoreceptor alignment. If this is so, then the guided component of the retinal reflectance should decrease when the photopigment is present in high optical density because much of the light passing through the outer segments will be absorbed by the photopigment. This prediction held for all three subjects tested in the bleaching experiment. The optimization routine was unable to find a guided component that accounted for a significant amount of the variance. Bleaching the retina increased the directionality of the retinal reflectance, restoring the variation in light intensity with pupil positions to that measured under the normal conditions (in which the photopigments are bleached). Two images

obtained for the deuteranomalous subject when the optics were in identical configurations are shown in Fig. 6. The only difference between these images is that one was obtained when the photopigments were present in high density [Fig. 6(a)] and the other was obtained after bleaching [Fig. 6(b)]. In the dark-adapted image only the first and the fourth Purkinje images are visible, along with a ghost reflection associated with the instrument that is located in the pupil at roughly eleven o'clock. We computed the density difference of the cone photopigments from the two measurements shown in Fig. 6 in a manner similar to other forms of retinal densitometry.^{16,31,35-39} Figure 7 shows density-difference contours for each point in the pupil for the data from Fig. 6. Note that near the peak of the bleached reflectivity distribution the density difference is greater than 0.4 for this individual. Maximum density differences measured for the three subjects who participated in the bleaching study ranged from 0.35 to 0.42.

B. Effect of Polarization

According to the research of van Bloklend, polarized light that has been guided by the photoreceptors remains polarized. In addition, the measured angle of polarization will be affected by the birefringence of the cornea and by the dichroism of the retinal nerve fiber layer. In contrast, light reflecting from the cornea-air interface will be polarized, but the angle of polarization should not vary over space. In Fig. 8 the effect of rotation of the analyzer over 180 deg on the intensity of reflected light is shown for three different exit locations in the pupil. For points at or near the peak of the guided component, as determined

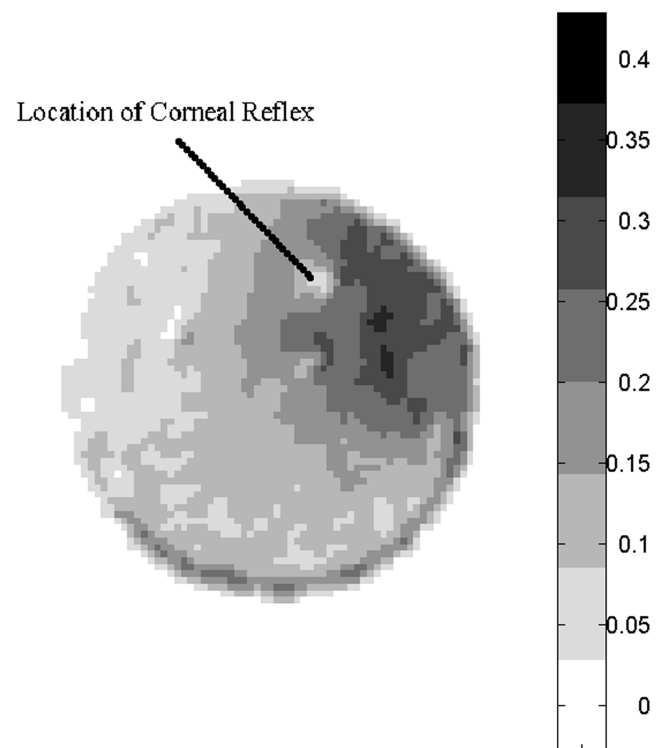


Fig. 7. Photopigment density difference computed for each point in the pupil from the intensity distributions shown in Fig. 6. The density difference is greatest in the region of the pupil where the bleached reflectance is highest.

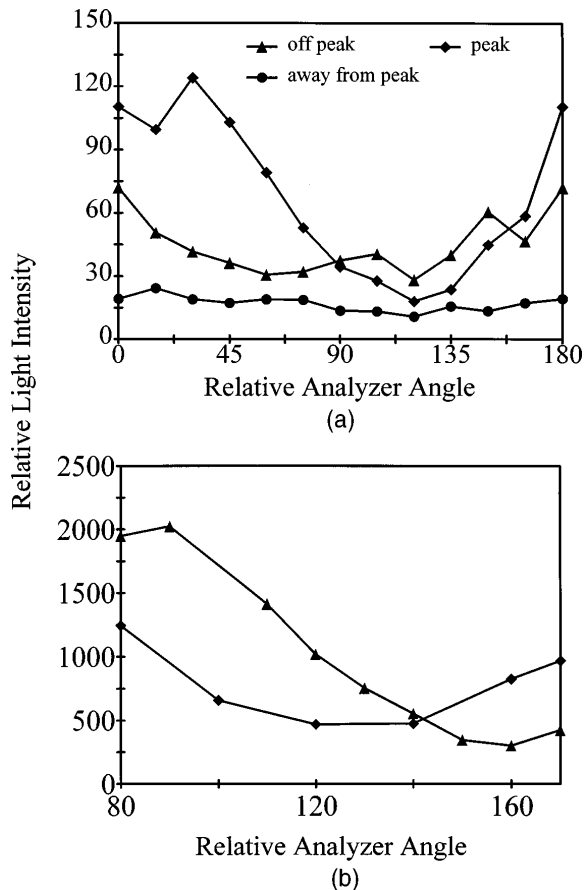


Fig. 8. Effect of changing the angle of a polarizer placed in the detection channel when the retina is illuminated with plane-polarized light. (a) For points near the peak of the guided component of the light there is a large change in reflectance with changes in the angle of the analyzer polarizer (\blacklozenge). For points farther from the peak of the photoreceptor alignment function there is less light emerging from the pupil, and there is less modulation of the light (\blacktriangle). Far from the peak (\bullet) there is little variation in the amount of light emerging from the pupil with changes in the angle of the analyzer, which suggests that this component of the light has been depolarized by multiple scattering. (b) Effect of changing the angle of the analyzer for different pupil positions. Data were collected with a longer sampling time and a higher degree of pixel binning (spatial averaging). These data show that the angle for which the minimum amount of light returns to the detector varies across the pupil. This variation is consistent with rotation of the polarized light by the birefringence of the cornea as the light passes through the cornea and back to the detector.

in the standard experiments, the intensity of the reflected light is strongly dependent on the angle of the analyzer, with a modulation of more than 0.85. However, far from the peak there is little change in the intensity with changes in the angle of the analyzer. This result was found for all three subjects tested in the polarization experiments. To test for variations in polarization with pupil entry position we increased the signal-to-noise level by increasing the integration time to 20 s and the amount of pixel binning to 8×8 . Figure 8(b) shows the relative angle that produces the minimal intensity for two different pupil exit positions, indicating that the light has been rotated differentially at different points in the pupil. The analyzer angle that produces the minimum intensity varies systematically across the pupil, with the largest ro-

tations occurring at the outer margin of the pupil.⁴⁰ Because retinal dichroism should contribute equally to every point in the pupil, this result is consistent with rotation of the plane-polarized light emerging from the pupil by corneal birefringence.

C. Retinal Imaging

Figure 9 is a retinal image taken with this apparatus. The large retinal vessels are readily visualized. In this image the subject is fixating the right-hand edge of the illuminated circle. To print this image we corrected for the variation in luminance across the image, but it accurately represents what is visible to the experimenter during the session. The circular reticle pattern is centered on the portion of the retina that is being tested and is inserted into the optical system in the plane of aperture A_2 (Fig. 2) when we move platform P_2 to permit retinal imaging. We control fixation by moving a retinal stop in the fixation channel (not depicted in Fig. 2, but see Gorrard and Delori²⁶).

4. DISCUSSION

A. Origin of the Directional Reflectance

Our goal was to develop a device to permit rapid optical measurement of photoreceptor alignment. The data support the hypothesis that the guided component of the measurements arises from the waveguide properties of the foveal cone photoreceptors. An alternative hypothesis is that the localization of light in the pupil is a result of specular reflections either from the retina or from anterior optical surfaces in the eye. Specular reflexes from the inner limiting membrane of the retina are readily visible in young eyes. There is strong evidence that we are not measuring the result of such a reflection in these experiments. First, we are able to measure a large change in the reflectivity of the retina with changes in photopigment concentration. Because this change is approximately 2.5:1 near the optimal pupil entry position, the contribution of a specular reflex from the inner limiting membrane is at most 40% of the light returning through the pupil in the bleached condition. The intensity and



Fig. 9. Image of the retina of subject SB that was obtained with the current apparatus. The subject is fixating the right-hand edge of the image. The concentric circles and the cross hairs are the image of a reticle located at position A_p . The center of the reticle is optically conjugate to the location of the measurement field.

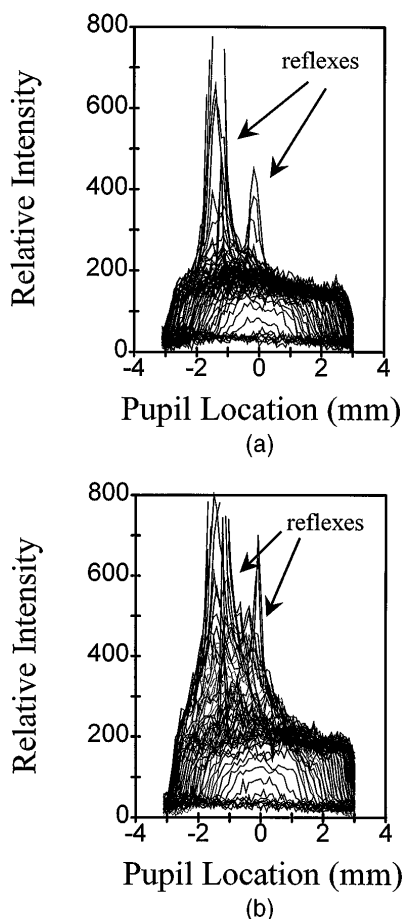


Fig. 10. Cross section of the data displayed as an image in Fig. 6. (a) Dark adapted, (b) light adapted. There is a large change in the relative reflectance of the retina with bleaching. This change is largest for a region near the peak of the high-illuminance reflectivity function in (b). Note that the intensities of the first and the fourth Purkinje reflexes are the same in both (a) and (b); they add a constant to the fundus reflectance measured in each image. This added constant will result in a decrease in the computed optical density of photopigments at the location of the reflexes. Similar results were obtained for three other subjects.

the uniform distributions of light in the dark-adapted pupil further reduce this estimate, although a uniform distribution can be predicted from measurements of the curvature of the human fovea.^{19,20} Figure 10 shows a plot of the intensity distribution of the pupil for the dark-adapted [Fig. 10(a)] and the bleached [Fig. 10(b)] data presented in Fig. 6. The maximum contribution to these data of a bleaching independent, uniformly distributed light (such as the reflection from the inner limiting membrane) is 20% of the peak measured when the photopigments are bleached. This value can be computed from the ratio of the maximum of the bleached distribution to the average dark-adapted intensity (the dark-adapted diffuse component). However, even this figure is an overestimate of the contribution of a specular reflex because, as we know from the polarization experiments, a large proportion of the diffuse component of the light emerging from the pupil is depolarized (Fig. 8). A reflection from the inner limiting membrane retains its polarization, although corneal birefringence may rotate the angle of polarization. Thus the majority of light that makes

up the diffuse component of the pupillary image cannot be originating from a reflection. We conclude that the total contribution of a reflection from the inner limiting membrane must be considerably less than 20%.

We can use similar arguments to counter the hypothesis that the variation in light measured across the pupil is due to the tails of the corneal reflex. Assume that some of the light is from the photoreceptors but that the tails of the corneal reflex are altering the intensity measurements. Light originating from layers anterior to the photopigments can only act to decrease the measured double density in a bleaching experiment. Thus the influence of the corneal reflex should be larger, and the measured density lower, the closer we are to the corneal reflex. Instead, the highest optical density is in the vicinity of the corneal reflex. Some contribution from the tails of the corneal reflex can be seen in the optical density contour map (Fig. 7), but the effect is small and localized and is therefore easily identified. The change in the distribution of light with bleaching (Fig. 10) also shows that the largest change in reflectivity with changes in photopigment concentration occurs in the area near the peak of the bleached intensity distribution.

The polarization studies also support the hypothesis that the light we are measuring is coming from behind the cornea. We find that the variation in intensity with the angle of the analyzer depends on the location in the pupil. Because all the measured light passes through a single region of the cornea on the way into the eye, and because we measure light only from a small region of the retina, variations in the angle of polarization across the pupil must result from light passing through different regions of the birefringent cornea. In fact, in some eyes we can detect the classic diamond pattern associated with birefringence of the cornea.⁴⁰ In an elegant study of the preservation of polarization of the light returning from the retina, van Blokland²⁴ showed that, whereas the portion of light that is guided by the photoreceptors retains its polarization, light that has been scattered more widely does not. We conclude from these data that the measured variation in the intensity of the pupil can be attributed to the photoreceptors preferentially guiding light along their axes, back toward the center of the pupil.

B. Shape of the Function

The computer-fitted space constant is narrower than the shape constant (defined similarly and expressed in inverse millimeters) that is measured in psychophysical experiments. Applegate and Lakshminarayanan³¹ found that the average value is 0.047 mm^{-2} , whereas the value obtained in this study is 0.083 mm^{-2} , roughly double that obtained psychophysically. Our values are similar to those obtained by van Blokland²³ and are roughly half those obtained by Gorrard and Delori²⁵ from some of the same subjects. The difference between the Gorrard–Delori study and the current study is that Gorrard and Delori scanned both the entrance and the exit pupils in tandem. Thus their measurements are affected by the directionality of the cones both for light traveling into the photoreceptors and for light emerging from the photoreceptors, which narrows the measured function, essentially squaring the distribution. Although the Gorrard–Delori technique is more sensitive to changes in the underlying

shape, it is not amenable to comparison of the retinal directionality obtained for different stimulus conditions.

The current estimates of the point in the pupil toward which the photoreceptors are optimally aligned agree with measurements of the Stiles–Crawford effect obtained from some of the same subjects.⁴¹ However, as mentioned above, the estimated space constants differ by a factor of roughly 2. There are two possible reasons for this discrepancy. First, psychophysical techniques are sensitive to the light that is absorbed within the photoreceptors. Chen and Makous⁴² showed that, for eccentric pupil entry positions, some of the psychophysical sensitivity arises from light that has emerged from the outer segment of one cone and has been absorbed by a neighboring cone. The reflectometric technique, however, measures primarily that portion of light that has passed through the outer segments twice. Thus the two techniques are sampling different portions of the light. The optical technique is sampling the photoreceptor antenna pattern, and the psychophysical technique is sampling the overall absorption of light. It has also been argued that, whereas the optical technique is maximally sensitive to a single mode of propagation of light through the photoreceptor waveguides, psychophysical measurements are sensitive to both propagated modes.^{2,25} A third possibility is that the optimal orientation of the photoreceptors varies across space.^{30,43} If so, then the measured directionality should depend on the entry pupil position. Although the current data cannot resolve these issues, the development of a rapid optical technique for measuring cone-photoreceptor orientation will allow us to address them in future studies.

ACKNOWLEDGMENTS

We thank Rob Webb for support and encouragement during this study. This research was supported by National Institutes of Health grants R01-EY04395 and R01-EY08511 (to F. Delori), by the Massachusetts Lions Eye Research Fund, and by the Chartrand Foundation.

REFERENCES

1. A. M. Laties and J. M. Enoch, "An analysis of retinal receptor orientation," *Invest. Ophthalmol. Vis. Sci.* **10**, 69–77 (1971).
2. A. W. Snyder and C. Pask, "The Stiles–Crawford effect—explanations and consequences," *Vision Res.* **13**, 1115–1137 (1973).
3. M. Mino and Y. Okano, "Improvement in the OTF of a defocused optical system through the use of shaded apertures," *Appl. Opt.* **10**, 2219–2225 (1971).
4. F. W. Campbell and R. W. Gubisch, "Optical quality of the human eye," *J. Physiol. (London)* **186**, 558–578 (1966).
5. G. Westheimer and F. W. Campbell, "Light distribution in the image formed by the living human eye," *J. Opt. Soc. Am.* **52**, 1040–1044 (1962).
6. F. Fankhauser, J. M. Enoch, and P. Cibis, "Receptor orientation in retinal pathology," *Am. J. Ophthalmol.* **52**, 767–783 (1961).
7. J. E. E. Keunen, V. C. Smith, J. Pokorny, and M. B. Mets, "Stiles–Crawford effect and color matching in Stargardt's disease," *Am. J. Ophthalmol.* **112**, 216–217 (1991).
8. P. H. Morse, V. C. Smith, J. Pokorny, and J. V. Burch, "Fundus flavimaculatus with cystoid macular changes and abnormal Stiles–Crawford effect," *Am. J. Ophthalmol.* **91**, 190–196 (1981).
9. V. C. Smith, J. Pokorny, and K. R. Diddie, "Color matching and the Stiles–Crawford effect in observers with early age-related macular changes," *J. Opt. Soc. Am. A* **5**, 2113–2121 (1988).
10. D. G. Birch, M. A. Sandberg, and E. L. Berson, "The Stiles–Crawford effect in retinitis pigmentosa," *Invest. Ophthalmol. Vis. Sci.* **22**, 157–164 (1982).
11. B. H. Crawford, "The Stiles–Crawford effects and their significance in vision," in *Visual Psychophysics, Handbook of Sensory Physiology*, D. Jameson and L. M. Hurvich, eds. (Springer-Verlag, Berlin, 1972), Vol. 7.
12. V. C. Smith, J. Pokorny, and K. R. Diddie, "Color matching and Stiles–Crawford effect in central serous choroidopathy," *Mod. Probl. Ophthalmol.* **19**, 284–295 (1978).
13. J. M. Enoch, J. A. van Loo, and E. Okun, "Realignment of photoreceptors in orientation secondary to retinal detachment," *Invest. Ophthalmol. Vis. Sci.* **12**, 849–853 (1973).
14. N. Bulow, "Light scattering by pigment epithelium granules in the human retina," *Acta Ophthalmol.* **46**, 1048–1053 (1968).
15. F. C. Delori and K. P. Pflibsen, "Spectral reflectance of the human ocular fundus," *Appl. Opt.* **28**, 1061–1077 (1989).
16. A. E. Elsner, S. A. Burns, G. W. Hughes, and R. H. Webb, "Reflectometry with a scanning laser ophthalmoscope," *Appl. Opt.* **31**, 3697–3710 (1992).
17. P. E. Kilbride, and K. M. Keehan, "Visual pigments in the human macula assessed by imaging fundus reflectometry," *Appl. Opt.* **29**, 1427–1435 (1990).
18. D. V. Norren and L. F. Tiemeijer, "Spectral reflectance of the human eye," *Vision Res.* **26**, 313–320 (1986).
19. J.-M. Gorrard, F. C. Delori, and D. M. Snodderly, "Specular reflection from the fovea," *Invest. Ophthalmol. Vis. Sci. Suppl.* **30**, 366 (1989).
20. D. R. Williams, "Visual consequences of the foveal pit," *Invest. Ophthalmol. Vis. Sci.* **19**, 653–667 (1980).
21. The interactions are considerably more complex than this simple model suggests. See Ref. 15.
22. J. Krauskopf, "Some experiments with a photoelectric ophthalmoscope," *Excerpta Med. Int. Congr. Ser.* (1965).
23. G. J. van Bloklant, "Directionality and alignment of the foveal receptors assessed with light scattered from the human fundus *in vivo*," *Vision Res.* **26**, 495–500 (1986).
24. G. J. van Bloklant and D. V. Norren, "Intensity and polarization of light scattered at small angles from the human fovea," *Vision Res.* **26**, 485–494 (1986).
25. J.-M. Gorrard and F. C. Delori, "A reflectometric technique for assessing photoreceptor alignment," *Vision Res.* **35**, 999–1010 (1995).
26. J.-M. Gorrard and F. C. Delori, "A method for assessing the photoreceptor directionality," *Invest. Ophthalmol. Vis. Sci. Suppl.* **31**, 425 (1990).
27. J.-M. Gorrard, "Directional effects of the retina appearing in the aerial image," *J. Opt.* **16**, 279–287 (1985).
28. W. S. Stiles and B. H. Crawford, "The luminous efficiency of rays entering the eye pupil at different points," *Proc. R. Soc. London Ser. B* **112**, 428–450 (1933).
29. W. S. Stiles, "The luminous efficiency of monochromatic rays entering the eye pupil at different points and a new colour effect," *Proc. R. Soc. London Ser. B* **123**, 90–118 (1937).
30. A. Safir and L. Hyams, "Distribution of cone orientations as an explanation of the Stiles–Crawford effect," *J. Opt. Soc. Am.* **59**, 757–765 (1969).
31. R. A. Applegate and V. Lakshminarayanan, "Parametric representation of Stiles–Crawford functions: normal variation of peak location and directionality," *J. Opt. Soc. Am. A* **10**, 1611–1623 (1993).
32. A. G. Bennett and J. L. Francis, "The eye as an optical system," in *The Eye*, H. Davson, ed. 2nd ed. (Academic, New York, 1962), Vol. 8, pp. 101–131.
33. "American National Standards for safe use of lasers," in ANSI 136 1-1993 (revision of ANSI 136 1-1986; Laser Institute of America, Orlando, Fla., 1993).
34. D. R. Williams, D. H. Brainard, M. J. McMahon, and R. Navarro, "Double-pass and interferometric measures of the optical quality of the eye," *J. Opt. Soc. Am. A* **11**, 3123–3135 (1994).
35. H. D. Baker, A. J. Watson, and D. C. Coile, "Experimen-

- tal stray light in retinal densitometry," *Vis. Neurosci.* **6**, 615–620 (1991).
36. D. V. Norren and J. van der Kraats, "A continuously recording retinal densitometer," *Vision Res.* **21**, 897–905 (1981).
 37. W. A. H. Rushton and G. H. Henry, "Bleaching and regeneration of cone pigments in man," *Vision Res.* **8**, 617–631 (1968).
 38. V. C. Smith, J. Pokorny, and D. V. Norren, "Densitometric measurement of human cone photopigment kinetics," *Vision Res.* **23**, 517–524 (1983).
 39. A. E. Elsner, S. A. Burns, and R. H. Webb, "Mapping cone pigment optical density in humans," *J. Opt. Soc. Am. A* **10**, 52–58 (1993).
 40. G. J. van Blokland, "The optics of the human eye with respect to polarized light," Ph.D. dissertation (Univ. of Utrecht, Utrecht, The Netherlands, 1986).
 41. S. A. Burns, A. E. Elsner, J.-M. Gorrard, M. R. Kreitz, and F. C. Delori, "Comparison of reflectometric and psychophysical measures of cone orientation," in *Noninvasive Assessment of the Visual System* Vol. 1 of 1992 OSA Technical Digest Series (Optical Society of America, Washington, D.C., 1992), pp. 160–163.
 42. B. Chen and W. Makous, "Light capture by human cones," *J. Physiol. (London)* **414**, 89–109 (1989).
 43. D. I. A. MacLeod, "Directionally selective light adaptation a visual consequence of receptor disarray?" *Vision Res.* **14**, 369–378 (1974).